



HAL
open science

Time-domain analysis of resonator array buffers

Yannick Dumeige

► **To cite this version:**

Yannick Dumeige. Time-domain analysis of resonator array buffers. IEEE Photonics Technology Letters, 2009, 21 (7), pp.435-437. 10.1109/LPT.2008.2012253 . hal-00474711

HAL Id: hal-00474711

<https://hal.science/hal-00474711>

Submitted on 5 Nov 2021

HAL is a multi-disciplinary open access archive for the deposit and dissemination of scientific research documents, whether they are published or not. The documents may come from teaching and research institutions in France or abroad, or from public or private research centers.

L'archive ouverte pluridisciplinaire **HAL**, est destinée au dépôt et à la diffusion de documents scientifiques de niveau recherche, publiés ou non, émanant des établissements d'enseignement et de recherche français ou étrangers, des laboratoires publics ou privés.



Distributed under a Creative Commons Attribution 4.0 International License

Time-Domain Analysis of Resonator Array Buffers

Yannick Dumeige

Abstract—We present design and time-domain simulations of microresonator array optical delay lines. The proposed buffer consists of an $n \times m$ microresonator array unidirectionally coupled via a straight bus waveguide. We show that the use of a two-dimensional arrangement of resonators can compensate for the high order of dispersion and more specifically the third-order dispersion. Numerical calculations confirm that pulses can be stored in microresonator arrays without appreciable distortion. Finally, we briefly describe the detrimental effects of optical losses and technological errors.

Index Terms—Coupled microresonators, optical delay lines.

INTEGRATED optical delay lines or buffers are key elements for a more complex system of optical signal processing. Different schemes have been proposed; among them, microresonator-based devices seem to provide a potential photonic circuit platform for this purpose [1]. The simplest and generic structure consists of a single lossless resonator used as an all-pass filter (APF) [2]. In this configuration, the resonator introduces only a phase shift ϕ in the incident field, as sketched in Fig. 1. Near its resonance angular frequency ω_0 , the APF is a very dispersive structure and $\phi(\omega)$ strongly depends on the angular frequency ω . Consequently, the APF allows optical pulses to be delayed by an amount given by the frequency-dependent group delay $\tau_g(\omega) = \partial\phi/\partial\omega$ (Fig. 1). The main limitation of this approach comes from the resonant feature of the delaying process [2]. Higher orders of dispersion β_p with $p > 1$, which are defined by $\beta_p = \partial^p\phi/\partial\omega^p$, strongly limit the bandwidth of the pulses that can be delayed without distortion. To circumvent this drawback, it has been proposed to use multistage APF by forming side-coupled integrated space sequence of resonators (SCISSOR) [3]. By using m identical resonators, the total delay is multiplied by m and the fractional delay is increased. Alternatively, it has been proposed to cascade APF whose properties are gradually tuned in order to flatten the group delay [2], [4]. Finally, Khurgin has suggested canceling high orders of dispersion by using arrays of coupled microresonators [5]. In this letter, we present design and time-domain performances of arrays of coupled microresonators used as optical buffers. We would like to highlight the interest of arrays of resonators and the main limitations of their practical use.

The proposed structure consists of an array of m identical columns of n single-mode microrings of radius R and effective index N_{eff} , as represented in Fig. 2(a). Each column of the array

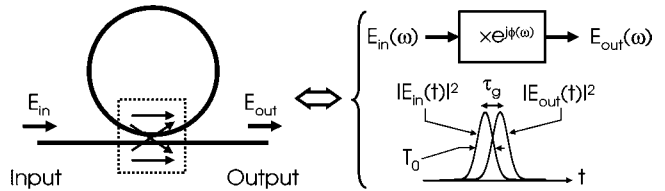


Fig. 1. Microresonator APF side coupled to a bus waveguide. The APF induces a phase shift $\phi(\omega)$ in an input field $E_{\text{in}}(\omega)$ and introduces a group delay τ_g on an optical pulse $E_{\text{in}}(t)$ of duration T_0 . The delayed pulse is noted $E_{\text{out}}(t)$.

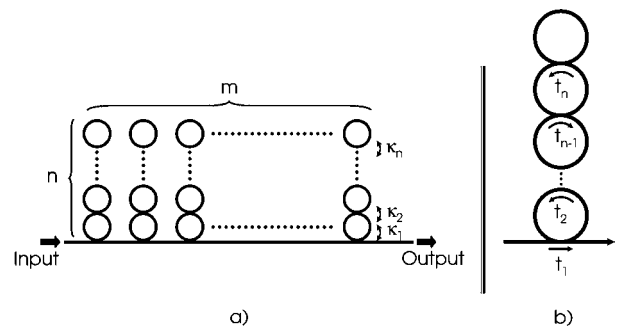


Fig. 2. (a) Microresonator array optical buffer and its bus waveguide. (b) Schematic representation of the unit cell.

represented in Fig. 2(b) is made up of a coupled resonator chain and unidirectionally coupled to others by the straight bus waveguide. For $n = 1$, we obtain an SCISSOR [3], and the case of $n = 2$ has been recently studied [6]. The coupling coefficients between resonators i and $i - 1$ for $i \in [2, n]$ is κ_i . ρ_i defined by $\rho_i^2 + \kappa_i^2 = 1$ is assumed real and positive. Similarly, the coupling coefficient between the bus waveguide and the first resonator is κ_1 . The amplitude transfer function of the unit cell is $t = \sqrt{T} \exp(j\phi) = t_1$ where we calculate t_1 by the recursive relation

$$t_i = \frac{\rho_i - t_{i+1} a \exp(j\varphi)}{1 - t_{i+1} \rho_i a \exp(j\varphi)} \quad (1)$$

where $a = \exp(-\alpha\pi R)$ and $\varphi = 2\pi N_{\text{eff}} R \omega / c$ are the round-trip amplitude attenuation and the phase shift. We define the frequency detuning δ by $\omega = \omega_0 + 2\pi\delta$. We will use a reference structure with $n = 1$, $R \approx 15.1 \mu\text{m}$, and $N_{\text{eff}} = 1.6$. With the coupling coefficient given in Table I, we obtain a maximal group delay $\tau_g(\delta = 0) = 6$ ps [see Fig. 3(a)]. As represented in Fig. 3(b), the third-order dispersion (β_3) at resonance ($\delta = 0$) for $n = 1$ is very strong and negative. This is the first limitation for pulse propagation since $\beta_2(0) = 0$ [5], [7]. It is possible to cancel $\beta_3(0)$ by using $n > 1$ resonators in the unit cell [8]–[11]. For $n = 2$, the line Config. 1 in Table I gives the coupling coefficients used to cancel $\beta_3(0)$ with a maximal delay at resonance

The author is with ENSSAT-FOTON (CNRS UMR 6082) Université de Rennes 1, 22300 Lannion, France (e-mail: yannick.dumeige@enssat.fr).

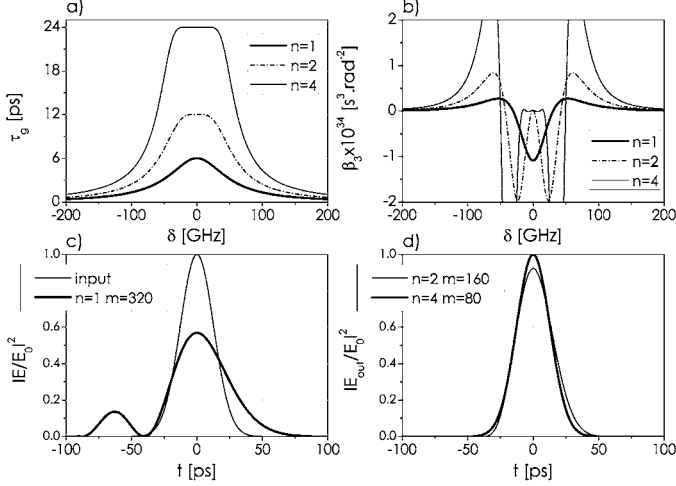


Fig. 3. (a) Group delay dispersion and (b) third-order dispersion introduced by the unit cell. (c) A 30-ps-long input pulse and output pulse delayed by about 1920 ps for $n = 1$. (d) Output pulses for the same input and the same delay as in (c) in the cases $n = 2$ and $n = 4$. In all the present calculations, we do not consider losses ($\alpha = 0$). For $n = 2$ and $n = 4$, we used the sets of coupling coefficients referring to Config. 1.

TABLE I

COUPLING COEFFICIENTS USED IN THE CALCULATIONS. CONFIGURATION 1 IS USED FOR $T_0 = 30$ ps AND CONFIGURATION 2 FOR $T_0 = 10$ ps

	κ_1	κ_2	κ_3	κ_4
$n = 1$	0.535j			
$n = 2$ Config. 1	0.630j	0.145j		
Config. 2	0.615j	0.141j		
$n = 4$ Config. 1	0.740j	0.233j	0.113j	0.074j
Config. 2	0.692j	0.203j	0.109j	0.076j

of 12 ps (twice the delay for $n = 1$). Fig. 3(a) and (b) also represents the group delay and the third-order dispersion for $n = 2$. In our time-domain simulations, we will also use $n = 4$ resonators. For $n > 2$, different ways can be adopted to cancel the third-order dispersion such as circuit-based methods [9]; here we used numerical optimization to calculate the values of the coupling coefficients $\mathbf{k} = (\kappa_1, \kappa_2, \dots, \kappa_n)$ of the unit cell. The objective function ε is defined by

$$\varepsilon(\mathbf{k}) = \sum_{\delta \in I} [\tau_0 - \tau_g(\delta, \mathbf{k})]^2 \quad (2)$$

where τ_0 is the targeted delay over a bandwidth B , then $I = [-B/2, B/2]$. By minimizing ε , we obtain a flat group delay for a bandwidth B which also leads to the cancellation of $\beta_3(0)$. The set of coefficients for $n = 4$ noted in Config. 1 has been calculated for $B = 40$ GHz and $\tau_0 = 24$ ps. The corresponding group delay and $\beta_3(\delta)$ are given in Fig. 3(a) and (b), respectively. Note that for each unit cell, we have chosen a maximal delay proportional to n in order to compare different structures with the same number of resonators $n \times m$ producing the same optical delay. We have simulated the performances of the different proposed structures in the time domain using the model described by Pereira *et al.* in [12] by assuming that the material dispersion is much weaker than the structural one. The calculation consists of the propagation of an input

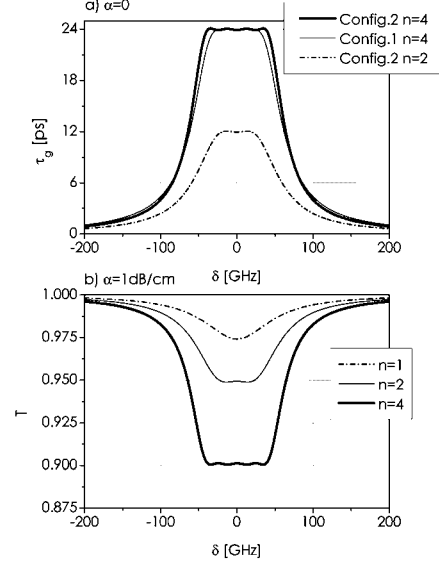


Fig. 4. (a) Group delay introduced by the unit cell for $n = 2$ and $n = 4$ in the lossless case of Config. 2; we also recall the group delay for $n = 4$ in the case of Config. 1. (b) Transmission of the unit cell with $\alpha = 1$ dB/cm; for $n = 2$ and $n = 4$, we used the second configuration.

Gaussian optical pulse of intensity profile $|E_{\text{in}}(t)|^2$ with an amplitude E_0^2 , an angular frequency $\omega_0 \approx 1.22 \times 10^{15}$ rad \cdot s $^{-1}$, and a full-width at half-maximum T_0 by a one-dimensional finite-difference method. First, we have chosen a total delay of 1.920 ns corresponding to 1×320 , 2×160 , and 4×80 $n \times m$ structures. For $T_0 = 30$ ps, the results are given in Fig. 3(c) and (d). The $n = 1$ structure strongly distorts the impulsion due to its strong negative β_3 . On the other hand, for the $n = 2$ and $n = 4$ structures, where the third-order dispersion has been canceled, the pulses are delayed without distortion. To show the real interest of using the $n = 4$ device, one has to use shorter pulses. With this in mind, we used pulses of temporal width $T_0 = 10$ ps. We used the same structures but for $n = 2$ and $n = 4$; we slightly changed the values of the coupling coefficients (keeping the same group delay) in order to increase their bandwidths. The corresponding coupling coefficients are given in Table I (see the line called ‘‘Config. 2’’). For $n = 4$, the optimization procedure has been used with $B = 80$ GHz and $\tau_0 = 24$ ps. Fig. 4(a) shows the group delay for the new unit cells for $n = 2$ and $n = 4$; we also recall the group delay dispersion for $n = 4$ with the previous set of coupling coefficient (Config. 1). In the two cases, the bandwidth has been increased and ripples appear in the group delay dispersion. For the time-domain simulations, we have chosen an overall delay of 120 ps; thus we used the following structures: 1×20 , 2×10 , and 4×5 . The thicker lines in Fig. 5(b)–(d) represent the simulation results. In the present example, the $n = 4$ structure induces less distortion than the $n = 2$ structure thanks to its larger bandwidth for the same delay per resonator. For $n = 1$, the pulse is still strongly distorted. In the lossless case, the simulations using the previous set of coefficients show a more pronounced distortion as represented in Fig. 5(c) and (d) in dashed–dotted lines. For structures compatible with short pulses ($T_0 = 10$ ps), we have studied the impact of optical

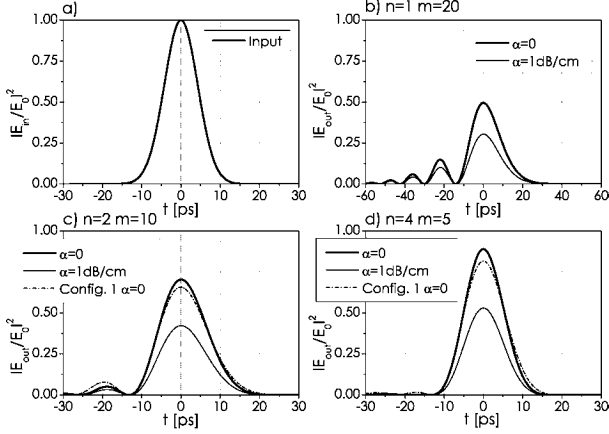


Fig. 5. (a) A 10-ps-long input pulse. Output pulses delayed by an amount of about 120 ps in the lossless case and for $\alpha = 1$ dB/cm: (b) $n = 1$, (c) $n = 2$, and (d) $n = 4$. For $n = 2$ and $n = 4$, we have used the second configuration; we also add the output pulses obtained with Config. 1 in the lossless case.

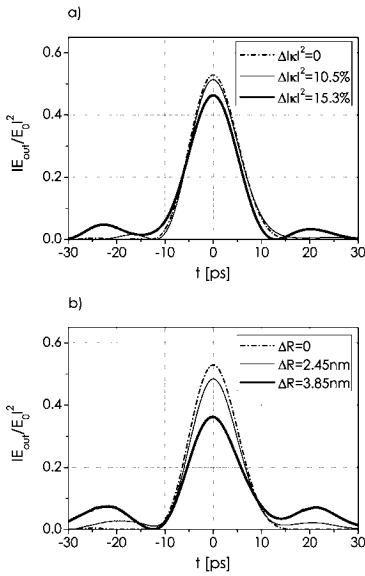


Fig. 6. Output pulses in the second configuration for $n = 4$ and $m = 5$ with losses $\alpha = 1$ dB/cm and technological errors: (a) considering errors of amplitude $\Delta |\kappa|^2$ in the intensity coupling coefficients; (b) considering errors of amplitude ΔR in the ring radius.

losses and technological errors. Fig. 4(b) represents the intensity transmission $T(\delta)$ of the different unit cells for losses equal to $\alpha = 1$ dB/cm. In this case, each unit cell not only introduces delay in the propagation but also optical losses. The temporal time-domain simulations given in Fig. 5(b)–(d) in thin lines show that low losses do not add distortion but only overall attenuation equal to $[T(\delta = 0)]^m$. This strongly limits in practice the use of high numbers of resonators. For insertion losses as high as 10 dB ($\alpha = 4.4$ dB/cm, $n = 4$, and $m = 5$), the pulses are not distorted using the same design. Note that for a given delay, the overall attenuation is the same for $n = 1$, $n = 2$, and $n = 4$ when the number of resonators is chosen. Finally, we have studied the impact of both technological errors in R and in the coupling coefficients on the temporal profile

of the output pulse. Fig. 6(a) represents the output pulse after propagation in a 4×5 structure where we added random deviation from the nominal values in the coupling coefficients. The mean maximal amplitude relative error is noted $\Delta |\kappa|^2$. These simulations show that errors up to 10% in the intensity coupling coefficients do not introduce too much additional distortion. We carried out the same calculations by adding random deviation to the values of the ring radii R with a maximal amplitude ΔR . The simulations presented in Fig. 6(b) show that errors about 4 nm in the radius size induce strong additional distortion in the output pulse profile. For our values of R and ω_0 , these errors give a resonance frequency mismatch around 50 GHz which is one order of magnitude larger than what is reported in [13].

We have performed time-domain simulations of microresonator array buffers. For a given resonator number $n \times m$ and a given overall delay, two lines of resonators ($n = 2$) are sufficient to cancel the third-order dispersion and to avoid pulse distortion for sufficiently long pulses. For shorter pulses, an increase in the number of lines allows the Gaussian shape of the input pulses to be preserved. The main limitations of such a buffer from a practical point of view come from optical losses and resonator size fabrication tolerance (better than 4 nm for an interference order about 100). In the chosen example, the relative coupling coefficient accuracy must be about 10%.

REFERENCES

- [1] F. Xia, L. Sekaric, and Y. Vlasov, "Ultracompact optical buffers on a silicon chip," *Nat. Photon.*, vol. 1, pp. 65–71, Jan. 2007.
- [2] G. Lenz, B. J. Eggleton, C. K. Madsen, and R. E. Slusher, "Optical delay lines based on optical filters," *IEEE J. Quantum Electron.*, vol. 37, no. 4, pp. 525–532, Apr. 2001.
- [3] J. E. Heebner and R. W. Boyd, "'Slow' and 'fast' light in resonator-coupled waveguides," *J. Mod. Opt.*, vol. 49, no. 14, pp. 2629–2636, 2002.
- [4] Z. Yang and J. E. Sipe, "Increasing the delay-time-bandwidth product for microring resonator structures by varying the optical ring resonances," *Opt. Lett.*, vol. 32, no. 8, pp. 918–920, Apr. 2007.
- [5] J. B. Khurgin, "Expanding the bandwidth of slow-light photonic devices based on coupled resonators," *Opt. Lett.*, vol. 30, no. 5, pp. 513–515, Mar. 2005.
- [6] L. Y. Mario and M. K. Chin, "Optical buffer with higher delay-bandwidth product in a two-ring system," *Opt. Express*, vol. 16, no. 3, pp. 1796–1807, Feb. 2008.
- [7] A. Melloni, F. Morichetti, and M. Martinelli, "Linear and nonlinear pulse propagation in coupled resonator slow-wave optical structures," *Opt. Quantum Electron.*, vol. 35, no. 4/5, pp. 365–379, 2003.
- [8] C. K. Madsen and G. Lenz, "Optical all-pass filters for phase response design with applications for dispersion compensation," *IEEE Photon. Technol. Lett.*, vol. 10, no. 7, pp. 994–996, Jul. 1998.
- [9] V. Van, "Circuit-based method for synthesizing serially-coupled microring filters," *J. Lightw. Technol.*, vol. 24, no. 9, pp. 2912–2919, Sep. 2006.
- [10] V. Van, T.-N. Ding, W. N. Herman, and P.-T. Ho, "Group delay enhancement in circular arrays of microring resonators," *IEEE Photon. Technol. Lett.*, vol. 20, no. 12, pp. 997–999, Jun. 15, 2008.
- [11] Y. Dumeige, T. K. N. Nguyen, L. Ghisa, S. Trebaol, and P. Féron, "Measurement of the dispersion induced by a slow-light system based on coupled active-resonator-induced transparency," *Phys. Rev. A*, vol. 78, pp. 013818 1–5, Jul. 2008.
- [12] S. Pereira, P. Chak, and J. E. Sipe, "Gap-soliton switching in short microresonator structures," *J. Opt. Soc. Amer. B*, vol. 19, no. 9, pp. 2191–2202, Sep. 2002.
- [13] T. Barwicz, M. A. Popovic, M. R. Watts, P. T. Rakich, E. P. Ippen, and H. I. Smith, "Fabrication of add-drop filters based on frequency-matched microring resonators," *J. Lightw. Technol.*, vol. 24, no. 5, pp. 2207–2218, May 2006.